

Infrared Intensity Study on Molecular Interactions in Quinhydrone

Isao Kanesaka,*[1] Hideyuki Nagami,[1] Kaori Kobayashi,[1] and Keiichi Ohno[2]

[1]Faculty of Science, Toyama University, 3190 Gofuku, Toyama 930-8555

[2]Graduate School of Science, Hiroshima University, 1-3-1 Kagamiyama, Higashi-Hiroshima 739-8526

Received July 5, 2005; E-mail: kanesaka@sci.toyama-u.ac.jp

The infrared intensities of the triclinic and monoclinic crystal modifications of quinhydrone (QH) have been measured, along with those of the parent molecules of *p*-hydroquinone (HQ) and *p*-benzoquinone (BQ) in solutions and in crystal form. The infrared spectra calculated by the density functional theory indicate that the hydrogen bond between HQ and BQ gives large changes in the infrared intensities of some bands of HQ, but gives rather small changes in the bands of BQ, even in ν(C=O). Charge-transfer interaction in QH is suggested to play an important role for the change in the infrared intensities of ν_{19a} at 1520 cm^{-1} and τ(C–H) at 530 cm^{-1} in HQ. In the two crystal modifications of QH, the hydrogen bond is stronger in triclinic QH than in monoclinic QH, whereas the electrostatic interaction is stronger in monoclinic QH than in triclinic QH. The intensity differences of BQ between the CCl_4 solution and the crystal are analyzed on the basis of the electrostatic model.

Recently, we have proposed an electrostatic model to account for the change in the infrared intensities of molecular vibrations in dielectric media, especially in the solid state.[1] In this model, changes in absolute intensity are assumed to originate from oscillating dipole moments induced by electric fields on the molecule or the effectively contributing functional group closely related to the normal mode. The infrared intensities of 1,10-dibromodecane in the urea clathrate and in the crystal have been analyzed in detail using this model.[1,2] In the present study, we will report the infrared intensities of quinhydrone (QH) as well as those of the parent compounds, *p*-hydroquinone (HQ) and *p*-benzoquinone (BQ), and discuss molecular interactions.

QH is the 1:1 molecular complex between HQ and BQ, and has triclinic and monoclinic crystal modifications, whose structures have been determined by Sakurai[3] and Sakurai[4] or Matsuda et al.,[5] respectively. In both kinds of crystals, O–H···O hydrogen bonds link the molecules to form infinite chains. The chains are stacked side by side in layers so that each molecule of a given chain is in charge-transfer (CT) interaction with two molecules of other species from the adjacent chains. In the triclinic crystal, all the hydrogen-bonded chains are parallel, whereas in the monoclinic crystal their orientation alternates from layer to layer.

The infrared and Raman spectra of the two crystal modifications of QH have been reported by Kubinyi and Keresztury.[6] They have studied molecular interactions by analyzing band shifts and deduced that CT interaction is very weak and spectral changes are due to the hydrogen bonds. Fukushima and Sakurada[7] have performed the normal coordinate analysis for the infrared active vibrations of monoclinic QH. In the present study, the infrared intensities of the two crystal modifications of QH, as well as those of the parent compounds in solutions and in the crystal, are measured and discussed on the basis of the hydrogen bond, electrostatic interactions, and CT interaction, by taking infrared spectra calculated by the density functional theory (DFT) into consideration.

Experimental

Triclinic QH was crystallized from a saturated ethyl acetate solution of equimolar HQ and BQ by bubbling N_2 gas.[3,6] Monoclinic QH was crystallized from a saturated aqueous solution of the equimolar parent molecules by slowly cooling from 60 to 30 °C.[6] The homogeneity of the two crystal modifications of QH was confirmed by the infrared bands at 1089/1078 cm^{-1} in triclinic/monoclinic QH.[6] BQ was purified by distillation under reduced pressure and the purity was confirmed by reference to infrared data.[8] HQ was used without purification. Infrared spectra were recorded at room temperature on a JASCO IR-810 spectrometer. Solid samples were mixed with KBr under N_2 and pressed into a disc. The observed infrared wavenumbers were calibrated by the use of those of polystyrene and are believed to be accurate within ± 2 cm^{-1}. The infrared intensity was obtained by measuring band areas and the local field correction for the solution sample was carried out by multiplying the factor, $9n/(n^2+2)^2$,[9] where n is the refractive index of the solvent (See Appendix A).

The theoretical calculations were performed using the Gaussian 03 program.[10] Optimal geometries, harmonic wavenumbers, and infrared intensities of single HQ and BQ, and hydrogen-bonded QH were calculated by DFT using the 6-311++G(3df,2pd) basis set. For DFT calculations, we used Becke's three-parameter exchange functional together with the correlation functionals of Lee–Yang–Parr (B3LYP). The atomic charges were taken from those for the atomic polar tensor (APT), which are used for calculating infrared intensities.[11]

Results and Discussion

Tables 1 and 3 summarize the absolute infrared intensities of some bands of HQ and BQ, respectively, in solutions and in crystal form, where ν, β, and τ are abbreviations of the stretching, in-plane bending, and out-of-plane bending vibrations, respectively. Tables 2 and 4 give the relative infrared intensity, I_R, of some bands of HQ and BQ in various states, respectively, where τ(C–H) at 800–900 cm^{-1}, which is less sensitive to molecular interactions, is used as the intensity

Published on the web March 8, 2006; DOI 10.1246/bcsj.79.406

Table 1. Absolute Infrared Intensities and Wavenumbers of Some Bands of HQ in the CH_3CN Solution and in the Crystal

Assignment	CH_3CN solution		Crystal		I_o^c/I_o^s
	ν/cm^{-1}	$I_o^{s\,a)}$	ν/cm^{-1}	$I_o^{c\,a)}$	
ν(C–C) + β(C–H)	1516	35.4	1518	30.9	0.9
ν(C–C) + β(O–H)	1455[b)]	<10.0[b)]	1472	58.5	>5
ν(C–O) + β(C–H)	1249	25.4	1251[c)]	31.8[d)]	1.3
β(O–H)	1214	88.9	1200[c)]	94.8[d)]	1.1
β(C–H)	1095	4.3	1095	5.1	1.2
τ(C–H)	833	26.3	827	33.8	1.3
β(C–C)	759	36.9	759	44.1	1.2
τ(C–H)	522	9.0	517	15.0	1.7

a) In 100 $cm^2\,mol^{-1}$. b) In the gaseous state.[17] c) Average of two bands. d) Sum of two bands.

Table 2. Observed and Calculated Relative Infrared Intensities, I_R, and Wavenumbers, ν/cm^{-1}, of Some Bands of HQ in Various States

	Obsd.					Calcd.			
		CH_3CN solution	Crystal	Triclinic QH	Monoclinic QH	Single HQ		Hydrogen-bonded QH	
Assignment	$\nu^{a)}$	I_R	I_R	I_R	I_R	ν	I_R	ν	I_R
ν(C–C) + β(C–H)	1520	2.45	1.59	1.12	1.03	1548	2.71	1551	2.98
ν(C–C) + β(O–H)	1478	<0.5[b)]	2.93	6.88	6.30	1488	1.40	1492	4.22
ν(C–O) + β(C–H)	1261	1.45	1.35[c)]	2.52	2.10	1249	2.95	1246	5.06
β(O–H)	1221	4.93	3.93[d)]	6.28	5.60	1176	4.46	1183, 1238	7.05
β(C–H)	1103	0.21	0.19	0.16	0.63	1116	0.70	1118	0.60
τ(C–H)	833	1.0	1.0	1.0	1.0	863	1.0[e)]	842	1.0[f)]
β(C–C)	762	1.28	1.44	1.12	0.90	750	0.79	755	0.81
τ(C–H)	530	0.21	0.26	0.72	0.67	518	0.38	520	0.24

a) Observed in triclinic QH. b) In the gaseous state. c) Two bands at 1260 and 1242 cm^{-1}. d) Two bands at 1209 and 1191 cm^{-1}. e) and f) The absolute values are 63.0 and 58.1 km mol^{-1}, respectively.

Table 3. Absolute Infrared Intensities and Wavenumbers of Some Bands of BQ in the CCl_4 Solution and in the Crystal

Species[a)]	Assignment	CCl_4 solution		Crystal		I_o^c/I_o^s
		ν/cm^{-1}	$I_o^{s\,b)}$	ν/cm^{-1}	$I_o^{c\,b)}$	
b_{1u}	ν(C=O)	1663[c)]	75.7	1660	86.6	1.2
b_{2u}	ν(C=C)	1592	3.9	1592	9.6	2.5
b_{1u}	β(C–H)	1357	2.5	1366	4.2	1.7
b_{2u}	ν(C–C) + β(C–H)	1302	16.4	1308	21.8	1.3
b_{2u}	β(C–H)	1066	13.1	1079	20.4	1.6
b_{1u}	β(C–C)	944	5.6	943	12.9	2.3
b_{3u}	τ(C–H)	884	37.5	903	40.7	1.1
b_{2u}	β(C=O)	409	24.5	417	34.9	1.4

a) In the D_{2h} symmetry. b) In 100 $cm^2\,mol^{-1}$. c) Average of two bands at 1670 and 1655 cm^{-1}.

Table 4. Observed and Calculated Relative Infrared Intensities, I_R, and Wavenumbers, ν/cm^{-1}, of Some Bands of BQ in Various States

		Obsd.					Calcd.			
			CCl_4 solution	Crystal	Triclinic QH	Monoclinic QH	Single BQ		Hydrogen-bonded QH	
Species[a)]	Assignment	$\nu^{b)}$	I_R	I_R	I_R	I_R	ν	I_R	ν	I_R
b_{1u}	ν(C=O)	1632	3.80	3.91	4.45	6.35	1725	6.26	1713, 1732	7.60
b_{2u}	ν(C=C)	1587	0.19	0.41	0.25	0.29	1643	0.23	1644	0.26
b_{1u}	β(C–H)	1363	0.10	0.16	—[c)]	—[c)]	1386	0.05	1392, 1402	0.06
b_{2u}	ν(C–C) + β(C–H)	1321	0.64	0.78	0.51	0.50	1316	1.03	1325	1.02
b_{2u}	β(C–H)	1089	0.42	0.60	0.25	0.33	1085	0.60	1094, 1177	0.90
b_{1u}	β(C–C)	951	0.16	0.33	0.23	0.15	912	0.21	921	0.30
b_{3u}	τ(C–H)	875	1.0	1.0	1.0	1.0	916	1.0[d)]	919	1.0[d)]
b_{2u}	β(C=O)	450	0.30	0.40	0.39	0.50	415	0.33	424	0.43

a) In the D_{2h} symmetry. b) In triclinic QH. c) Overlapping with the bands of HQ. d) The absolute value is 73.3 km mol^{-1} in both states.

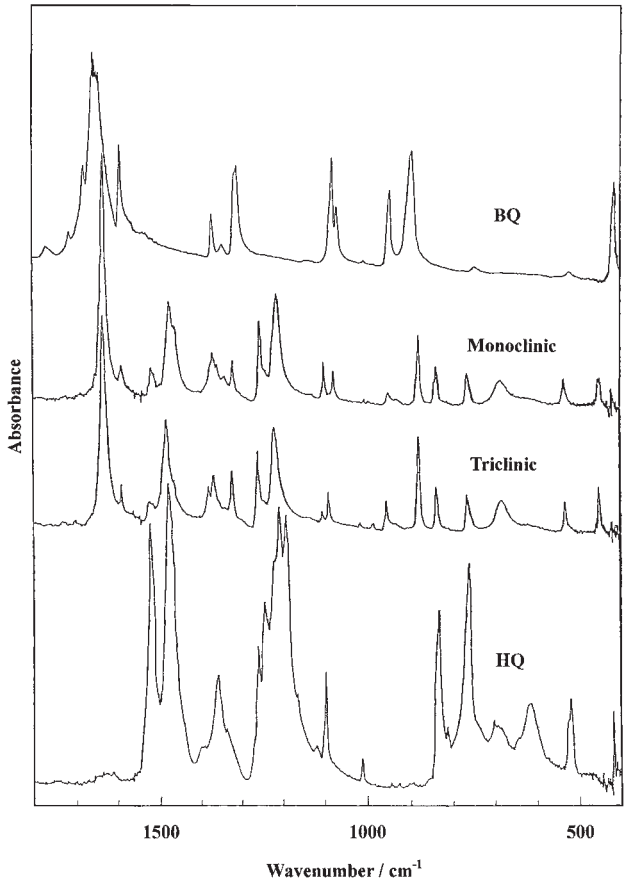

Fig. 1. Observed infrared spectra of HQ, BQ, and two modifications of QH in the crystal.

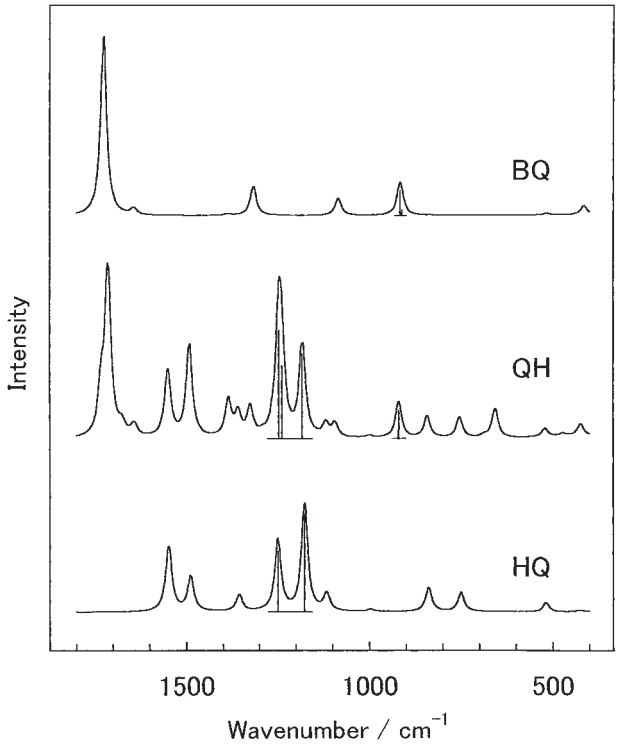

Fig. 2. Infrared spectra calculated by the B3LYP/6-311++G(3df,2pd) level. QH has a co-planar structure forming a hydrogen bond.

standard. The observed bands are assigned by reference to the normal modes calculated by the B3LYP/6-311++G-(3df,2pd) level; they coincide with the assignments reported by Becker et al.[12–14] for BQ and by some authors[15,16] for HQ.

The infrared spectra of the two crystal modifications of QH are given in Fig. 1, along with those of HQ and BQ in the crystal. Although the wavenumbers of the observed bands in the two crystal modifications of QH correlate well to those of HQ and BQ in the crystal, except for the 1400–1300 cm^{-1} region, considerable changes in infrared-band intensity are seen in Fig. 1. For example, in two bands of HQ at 1520 and 1478 cm^{-1}, which are so-called ν_{19a} and ν_{19b}, respectively, the intensity of the former markedly decreases and that of the latter increases in the two crystal modifications of QH. It is known for HQ that in the gaseous state the intensity of ν_{19a} is significantly stronger than that of ν_{19b}.[17]

Figure 2 shows the calculated spectra by DFT for single HQ and BQ, and hydrogen-bonded QH, where QH has a co-planar structure. Hence, the symmetry of HQ and BQ in hydrogen-bonded QH is lowered and the spectrum of hydrogen-bonded QH becomes complicated. The calculated intensity of ν_{19b} increases by about 3 times in hydrogen-bonded QH compared to that in single HQ, whereas the intensity of ν_{19a} changes slightly. The calculated intensity of ν(C–O) at 1230 cm^{-1} increases in hydrogen-bonded QH, which results from overlapping with β(O–H) and the complex coupling between β(O–H) and ν(C–O) due to the lowering of the symmetry. The calculated intensity of τ(C–H) at 518 cm^{-1} in hydrogen-bonded QH decreases considerably due to the hydrogen bond, although a large increase is found in the two crystal modifications of QH compared to the CH_3CN solution. Thus, this increase in intensity is not attributed to the hydrogen bond. Foucrault et al.[18] have discussed the stacked structure of QH by the nonempirical calculation. However, the optimized structure differs largely from the real one.

Infrared-Band Intensities of HQ in the CH_3CN Solution, Crystal, and QH. Table 1 shows the absolute infrared intensity of some bands of HQ in the CH_3CN solution and in the crystal. Since the α crystal form of HQ has a complex structure with 56 molecules in the unit cell ($z = 56$),[19] complicated interactions may occur. ν_{19b} in the crystal increases by >5 times compared to that in the gaseous state.[17] This increase is explained in terms of the hydrogen bond by reference to Fig. 2. On the other hand, the intensity of ν_{19a} decreases somewhat in the crystal.

Table 2 shows the relative infrared intensities, I_R, of some bands of HQ in various states, where I_R and the wavenumbers calculated by DFT are also given. In this case, τ(C–H) at 833 cm^{-1} is used as the intensity standard. The DFT calculations indicate that the increases of I_R of the three bands at 1478 (ν_{19b}), 1261 and 1221 cm^{-1} in triclinic QH, compared with those in the CH_3CN solution are explained in terms of the hydrogen bond. On the other hand, the noticeable increase of the I_R of τ(C–H) at 530 cm^{-1} and the decrease in ν_{19a} in the two crystal modifications of QH compared with the CH_3CN solution are not explained in terms of the hydrogen bond. Hence, their large changes may result from electrostatic interactions and/or CT interaction. These will be discussed below.

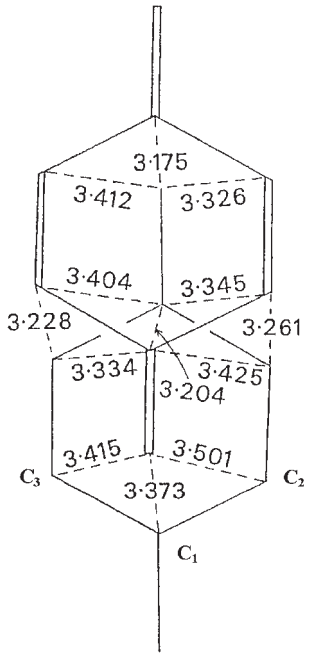

Fig. 3. Interatomic distances[3] in Å between molecular chains in triclinic QH. Upper molecule: BQ; lower molecule: HQ.

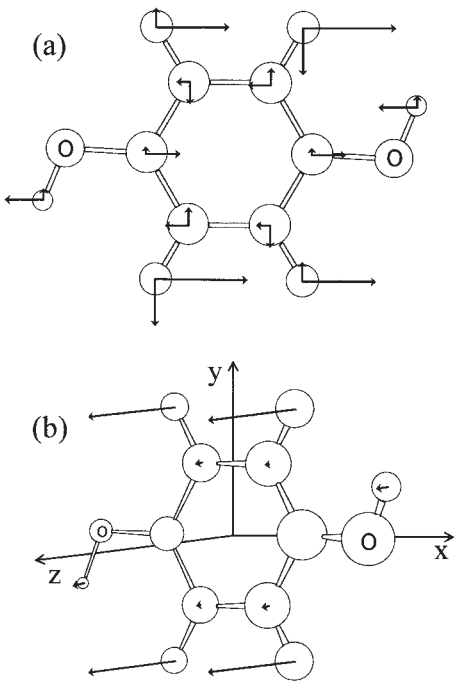

Fig. 4. The vibrational modes of ν_{19a} (a) and τ(C–H) (b).

Figure 3 shows the interatomic distances between HQ and BQ in triclinic QH.[3] According to the electrostatic model,[1] (See also Appendix A) the electric field at the C_1–C_2 and C_1–C_3 bonds of HQ generated by BQ may change the intensity of ν_{19a} by reference to the normal mode (See Fig. 4a). The electrostatic potential, ϕ, at three carbon atoms, C_1, C_2, and C_3, is roughly estimated by use of the APT atomic charges of the C=O bond, ε_O and ε_C (see Fig. 5a), neglecting other atomic charges, as

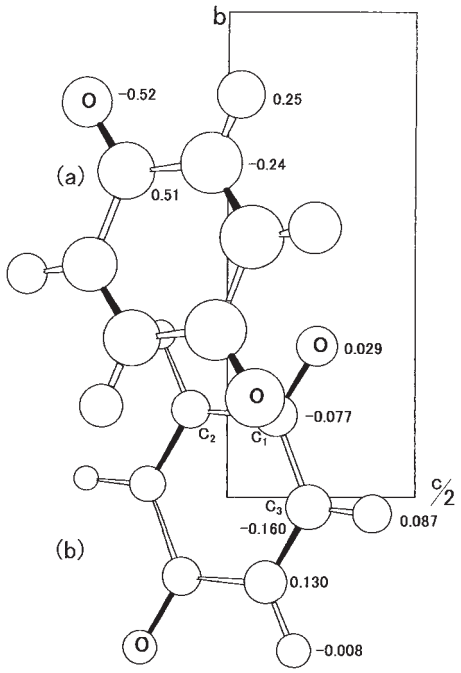

Fig. 5. Crystal structure of BQ. (a): APT atomic charges in the electron unit; (b): electrostatic potentials in e Å^{-1}.

$$\phi_i = \frac{\varepsilon_o}{r_{(C_i\text{–}O)}} + \frac{\varepsilon_c}{r_{(C_i\text{–}C)}}, \quad (1)$$

where r is the atomic distance between C_i and O or C in BQ. The values of ϕ_{C1}, ϕ_{C2}, and ϕ_{C3} are 0.042, 0.040, and 0.029 e Å^{-1} (Å $= 10^{-10}$ m), respectively, where e is the elementary electric charge. The value of the Raman tensor, α_1, defined in Appendix A, is evaluated to be 0.081 Å^3 by reference to $\partial\alpha/\partial r_{C\text{–}C}$, 1.88 Å^2, in benzene.[20] The induced oscillating dipole moments, $\alpha_1 E_R$ ($E_R = (\phi_i - \phi_j)/r_{ij}$), are 0.001 and 0.004 D (D = e cm/4.8) for the C_1–C_2 and C_1–C_3 bonds, respectively. Since the intrinsic value of μ_1 of ν_{19a} in the CH_3CN solution is 0.12 D (See Appendix A), the observed large decrease on going from the CH_3CN solution to the two crystal modifications of QH is not explained in terms of the electrostatic model: $m_1 = \mu_1 + \sum \alpha_1 E_R$, where $\sum$ means the sum of four bonds. Although E_R may be modified, considering the electric field at the position of the atom, as shown later, an increase in $\alpha_1 E_R$ is not expected because the modified electric field is generally less than that defined above. Hence, the large decrease in the infrared intensity observed for ν_{19a} in the two crystal modifications of QH compared to the CH_3CN solution may be due to CT interaction, by referring that the quantity of CT has been evaluated 0.04 e from SCF calculation[18] and 0.21 e/0.71 e in triclinic/monoclinic QH from X-ray studies.[3,4]

The increase of the I_R of τ(C–H) at 530 cm^{-1} on going from the CH_3CN solution to the two crystal modifications of QH is not due to the change of the C–H bond moments by electrostatic interactions, because the I_R of τ(C–H) at 833 cm^{-1} does not change largely. Since the increase in the intensity is not also due to the hydrogen bond, as described above, the increase may be due to CT interaction, by referring that the directions of CT and the vibrational transition moment are parallel to each other. The normal mode of τ(C–H) at 530 cm^{-1} is given in Fig. 4b.

In Table 2, the intensity of the I_R of β(C–H) at 1103/1102 cm^{-1} is 0.16/0.63 in triclinic/monoclinic QH, which shows the largest difference. However, the reason is obscure.

Infrared-Band Intensities of BQ in the CCl_4 Solution, Crystal, and QH. Table 3 shows the absolute intensities of some bands of BQ in the CCl_4 solution and in the crystal. The present spectrum of BQ in the crystal in Fig. 1 coincides with the reference data,[8] but it differs markedly with that reported by Davies and Prichard.[21] In Table 3, the absolute intensities in the crystal are as a whole stronger than those in the CCl_4 solution (See Appendix A), especially for ν(C=C) at 1592 cm^{-1} and β(C–C) at 944 cm^{-1}, whose intensities increase by 2.5 and 2.3 times, respectively. The band intensities at 1357 and 1066 cm^{-1} also increase considerably. These increases may result from electrostatic interactions in the crystal, which will be discussed later.

Table 4 shows the relative intensity, I_R, of some bands of BQ in various states, where τ(C–H) at 875 cm^{-1} is used as the intensity standard, and I_R and the wavenumbers calculated by DFT are also given. The DFT calculations of BQ in single BQ and hydrogen-bonded QH almost reproduce the observed changes in infrared intensity, except for β(C–H) at 1089 cm^{-1}. That is, the intensity changes from the CCl_4 solution to the two crystal modifications of QH are mostly due to the hydrogen bond. On the other hand, considerable changes in I_R between the two crystal modifications of QH are observed. The intensity of the I_R of ν(C=O) at 1632/1632 cm^{-1} is 4.45/6.35 in triclinic/monoclinic QH. According to the electrostatic model[22] (See also Appendix B), the lower shift of ν(C=O) from 1663 (CCl_4) to 1632 (crystal) cm^{-1} depends on both the strength of the hydrogen bond and the dipole moment derivative of the C=O stretching, $\partial\mu/\partial r$. Hence, the lower shift by $\partial\mu/\partial r$ is larger in monoclinic QH than in triclinic QH by reference to the observed intensity. In other words, the hydrogen bond in triclinic QH is stronger than that in monoclinic QH, since the total lower shift by both effects is the same in each QH. This is supported by the wavenumbers of the bands of HQ relating to the hydrogen bond as 1478/1470 and 1221/1213 cm^{-1} in triclinic/monoclinic QH, although ν(O–H) is observed at 3232/3223 cm^{-1}.

The intensity of the I_R of β(C–C) at 951/945 cm^{-1} in triclinic/monoclinic QH is 0.23/0.15. The calculated intensity of β(C–C) increases in hydrogen-bonded QH compared with that of single BQ. This is mainly due to the vibrational coupling with β(C–H) at 1089 cm^{-1}. The sum of the I_R of 1089 and 951 cm^{-1} in triclinic QH is the same as that in monoclinic QH, as realized in Table 4. This indicates that the differences in the I_R of both β(C–C) and β(C–H) between the two crystal modifications of QH are due to the vibrational coupling of β(C–C) and β(C–H).

As described above, the intensity change of BQ in Table 3 on going from the CCl_4 solution to the crystal may be due to electrostatic interactions. Figure 5 shows the crystal structure of BQ,[23] which belongs to the space group of $C_{2h}{}^5 \equiv P2_1/a$ with $z = 2$. APT atomic charges are shown in Fig. 5a. Figure 5b shows the values of ϕ, which are obtained by taking the summation from atomic charges in the region of $r \leq 50$ Å. The increase of the infrared intensity of ν(C=C), 2.5 times, on going from the CCl_4 solution to the crystal is mainly discussed below. In this case, the value of α_1 is evaluated to be 0.12 $Å^3$ by reference to the Raman intensity of ν(C=C) of vinyl acetylene.[20] Since E_R can be calculated as 0.22 e $Å^{-2}$ from ϕ in Fig. 5b, the resulting value of $\alpha_1 E_R$ is 0.12 D. However, this results in the large enhancement, 17 times, by referring that the intrinsic transition moment, μ_1,[1,24] is 0.039 D in the CCl_4 solution (See Appendix A). The discrepancy between the observed and evaluated enhancements may be an overestimation of E_R. In a molecule, the electric field applied not to the bond, but to the atom may be important for the induced dipole moment, because the polarizability is defined on the atom, as discussed by analysis of the Raman intensity.[25–27] This means that the effective electric field for the induced dipole moment is not E_R described above, but the electric field on each atom, $\bar{E}_R{}^a$. $\bar{E}_R{}^a$ may differ, sometimes, completely with E_R; for example, the potential on the C_2' atom in Fig. 5b is the maximum surrounded by negative values in three atoms, suggesting that $\bar{E}_R{}^a \approx 0$. $\bar{E}_R{}^a$ on the C_2' atom along the C_2–C_3 bond may be obtained by taking the summation of E_R along the C_2–C_3 bond as $\boldsymbol{E}_R(C_3\text{–}C_2') + \boldsymbol{E}_R(H\text{–}C_2') + \boldsymbol{E}_R(C_1\text{–}C_2')$, i.e., -0.006 e $Å^{-2}$. Similarly, $\bar{E}_R{}^a$ on the C_3 atom along the C_2–C_3 bond is 0.11 e $Å^{-2}$. Since α_1 may result equivalently from two carbon atoms, the electric field for the bond may be averaged as $\bar{E}_R{}^b = \{(\bar{E}_R{}^a(C_2') + \bar{E}_R{}^a(C_3)\}/2$; $\bar{E}_R{}^b$ is 0.054 e $Å^{-2}$ and this gives $\alpha_1 \bar{E}_R{}^b = 0.029$ D, which results in an enhancement by 3.0 times. Hence, the observed enhancement is almost explained in terms of the electrostatic model. Since β(C–C) at 944 cm^{-1} is regarded as the rotational mode of the C=C bonds, the increase of I_R is also explained in terms of the induced dipole moment on the C=C bonds as $\alpha\bar{E}_R{}^b = 0.43$ D, where the polarizability of the C=C bond α is 1.65 $Å^3$.[28]

Appendix

A. Infrared Intensity and Related Items. The definition of the infrared intensity and relating items are summarized to understand well the results given in Tables 1–4. The absolute infrared intensity is defined as[24]

$$\Gamma_a = \frac{8\pi^3}{3hc} N_a m_1{}^2, \tag{A-1}$$

where h is the Planck constant, c the velocity of light, N_a the Avogadro constant, and m_1 the transition dipole moment. The correction by the local radiation field in the liquid state is given as[9,29]

$$\Gamma_o = \Gamma_a(E_l/E_\infty)^2/n = \Gamma_a(n^2+2)^2/9n, \tag{A-2}$$

where E_l and E_∞ are the local radiation field and macroscopic field, respectively. Γ_o in $cm^2\,mol^{-1}$ is obtained as

$$\Gamma_o = \frac{1000}{\nu_0}\int \frac{A}{c'l}\,d\nu, \tag{A-3}$$

where A is the absorbance, ν_0 the peak position in cm^{-1}, c' the concentration in mol cm^{-3}, and l the length of a cell in cm. Γ_o' in cm mol^{-1} or km mol^{-1} is defined as

$$\Gamma_o' = 1000\int \frac{A}{c'l}\,d\nu, \tag{A-4}$$

which is used in a simulation of spectra.

The transition dipole moment m_1 in Eq. A-1 is given by the electrostatic model as[1,22]

$$m_1 = \mu_1 + \alpha_1 E_R, \tag{A-5}$$

where μ_1 and α_1 are the intrinsic transition moment and the Raman tensor, respectively, which is defined as

$$\gamma_1 = \frac{\partial \gamma}{\partial Q}\langle 1|Q|0\rangle, \tag{A-6}$$

where $\gamma_1 = \mu_1$ or α_1.

In Eq. A-5, E_R is the electric field on the oscillator. In the liquid state, E_R due to the permanent dipole moment of a molecule, μ_p, is given as[21,29,30]

$$E_R = \frac{\varepsilon_s - 1}{2\varepsilon_s + 1}\frac{2\mu_p}{a^3}, \tag{A-7}$$

where ε_s is the static dielectric constant of the solution and a the radius of a molecule assumed to be a sphere. E_R in the solid state is evaluated by use of the electrostatic potential, ϕ, generated by point charges, as done in the present study. The other methods to evaluate E_R by use of bond moments, or dipole moments, are as follows. Interaction energy, I, among bond moments is given as

$$I = \sum_j \mu_0 \mu_j \frac{\cos\gamma_{0j} - 3\cos\gamma_0 \cos\gamma_j}{{r_{0j}}^3}, \tag{A-8}$$

where r_{0j} is the distance between the bond moments of μ_0 and μ_j, γ_{0j} the angle between μ_0 and μ_j, γ_0 the angle between μ_0 and r_{0j}, and γ_j the angle between μ_j and r_{0j}. E_R is obtained as

$$E_R = I/\mu_0. \tag{A-9}$$

In the crystal, Eq. A-5 is further modified as[1]

$$m_1 = \mu_1 + \alpha_1 E_R + \frac{4\pi\alpha m_1}{3V}, \tag{A-10}$$

where the last term is the oscillating dipole moment due to the oscillating polarization, m_1/V (V: the volume of a unit cell), and the effective polarizability of an oscillator, α.

B. Band Shift Due to a Hydrogen Bond. An electrostatic model of the band shift in the hydrogen-bonded system is reviewed, because no applicable formulation has been reported. We consider the interaction potential energy acting on the C=O bond in the hydrogen-bonded system, –OH···O=C<, assuming that the ionic structure of the OH bond contributes to hydrogen bond, i.e., the interaction between the point charge of the hydrogen atom, q_o, and the dipole of the C=O bond.[31] The interaction potential energy is obtained as

$$U = -\frac{q_o \mu_e \cos\theta}{r^2}, \tag{A-11}$$

where μ_e is the bond moment of the C=O bond, r is the distance between the hydrogen atom and an effective site of the C=O bond, and θ is the angle between r and the C=O bond. The internal coordinate of the C=O bond, ξ, may be related to r by the equation

$$r = r_o - \xi\cos\theta. \tag{A-12}$$

Thus, if we expand U as

$$U = U_o + U'\xi + U''\xi^2/2 + \ldots, \tag{A-13}$$

U' and U'' are given as

$$U' = \frac{\partial U}{\partial \xi} = -\frac{2q_o\mu_e\cos^2\theta}{{r_o}^3} - \frac{q_o{\mu_e}'\cos\theta}{{r_o}^2}, \tag{A-14}$$

where ${\mu_e}' = \partial\mu_e/\partial\xi$ and

$$U'' = \frac{\partial^2 U}{\partial \xi^2} \approx -\frac{6q_o\mu_e\cos^3\theta}{{r_o}^4} - \frac{4q_o{\mu_e}'\cos^2\theta}{{r_o}^3}. \tag{A-15}$$

Upon applying the perturbation theory to Eq. A-13 and adopting the cubic term in the potential function of ν(C=O), k', the wavenumber shift for the fundamental is given in cm^{-1} as[22]

$$\Delta\nu = \left(\frac{U''}{2\gamma} - \frac{3k'U'}{2\gamma^2 h\nu}\right)/hc, \tag{A-16}$$

where

$$\gamma = 4\pi^2\nu m^*/h. \tag{A-17}$$

Here, m^* is the reduced mass assuming the C=O group as a diatomic species and ν is the harmonic frequency. Equation A-16 indicates that $\Delta\nu$ depends on both the strength of the hydrogen bond, q_o and r_o, and the square route of the intensity, ${\mu_e}'$.

References

1 I. Kanesaka, *Spectrochim. Acta, Part A* **2004**, *60*, 297.
2 I. Kanesaka, S. Matsuzawa, T. Ishioka, Y. Kitagawa, K. Ohno, *Spectrochim. Acta, Part A* **2004**, *60*, 2621.
3 T. Sakurai, *Acta Crystallogr.* **1965**, *19*, 320.
4 T. Sakurai, *Acta Crystallogr., Sect. B* **1968**, *24*, 403.
5 H. Matsuda, K. Osaki, I. Nitta, *Bull. Chem. Soc. Jpn.* **1958**, *31*, 611.
6 M. Kubinyi, G. Keresztury, *Spectrochim. Acta, Part A* **1989**, *45*, 421.
7 K. Fukushima, M. Sakurada, *J. Phys. Chem.* **1976**, *80*, 1367.
8 C. J. Pouchert, *The Aldrich Library of Infrared Spectra*, Aldrich Chemical, Milwaukee, **1981**.
9 S. R. Polo, M. K. Wilson, *J. Chem. Phys.* **1955**, *23*, 2376.
10 M. J. Frisch, G. W. Trucks, H. B. Schlegel, G. E. Scuseria, M. A. Robb, J. R. Cheeseman, J. A. Montgomery, Jr., T. Vreven, K. N. Kudin, J. C. Burant, J. M. Millam, S. S. Iyengar, J. Tomasi, V. Barone, B. Mennucci, M. Cossi, G. Scalmani, N. Rega, G. A. Petersson, H. Nakatsuji, M. Hada, M. Ehara, K. Toyota, R. Fukuda, J. Hasegawa, M. Ishida, T. Nakajima, Y. Honda, O. Kitao, H. Nakai, M. Klene, X. Li, J. E. Knox, H. P. Hratchian, J. B. Cross, C. Adamo, J. Jaramillo, R. Gomperts, R. E. Stratmann, O. Yazyev, A. J. Austin, R. Cammi, C. Pomelli, J. W. Ochterski, P. Y. Ayala, K. Morokuma, G. A. Voth, P. Salvador, J. J. Dannenberg, V. G. Zakrzewski, S. Dapprich, A. D. Daniels, M. C. Strain, O. Farkas, D. K. Malick, A. D. Rabuck, K. Raghavachari, J. B. Foresman, J. V. Ortiz, Q. Cui, A. G. Baboul, S. Clifford, J. Cioslowski, B. B. Stefanov, G. Liu, A. Liashenko, P. Piskorz, I. Komaromi, R. L. Martin, D. J. Fox, T. Keith, M. A. Al-Laham, C. Y. Peng, A. Nanayakkara, M. Challacombe, P. M. W. Gill, B. Johnson, W. Chen, M. W. Wong, C. Gonzalez, J. A. Pople, *Gaussian 03, Revision B.05*, Gaussian, Inc., Pittsburgh PA, **2003**.
11 M. M. C. Ferreira, *J. Phys. Chem.* **1990**, *94*, 3220.
12 E. Charney, E. D. Becker, *J. Chem. Phys.* **1965**, *42*, 910.
13 H. Ziffer, E. Charney, E. D. Becker, *J. Chem. Phys.* **1965**, *42*, 914.
14 E. D. Becker, *J. Phys. Chem.* **1991**, *95*, 2818.
15 A. Hidalgo, C. Otero, *Spectrochim. Acta* **1960**, *16*, 528.
16 R. J. Jakobsen, E. J. Brewer, *Appl. Spectrosc.* **1962**, *16*, 32.
17 H. W. Wilson, *Spectrochim. Acta, Part A* **1974**, *30*, 2141.
18 M. Foucrault, P. Hobza, C. Sandorfy, *THEOCHEM* **1987**, *152*, 11.

19 S. C. Wallwork, *J. Chem. Soc., Perkin Trans. 2* **1980**, 641.
20 H. W. Schrotter, H. J. Bernstein, *J. Mol. Spectrosc.* **1964**, *12*, 1.
21 M. Davies, F. E. Prichard, *Trans. Faraday Soc.* **1963**, *59*, 1248.
22 A. D. Buckingham, *Proc. R. Soc. London, Ser. A* **1958**, *248*, 169.
23 J. Trotter, *Acta Crystallogr.* **1960**, *13*, 86.
24 G. Turrell, *Infrared and Raman Spectra of Crystal*, Academic Press, London, **1972**.
25 I. Kanesaka, S. Ikeda, *J. Raman Spectrosc.* **1992**, *23*, 181.
26 I. Kanesaka, T. Matsuda, Y. Niwa, *J. Raman Spectrosc.* **1994**, *25*, 245.
27 I. Kanesaka, T. Matsuda, Y. Morioka, *J. Raman Spectrosc.* **1995**, *26*, 239.
28 K. J. Miller, *J. Am. Chem. Soc.* **1990**, *112*, 8533.
29 H. Frolich, *Theory of Dielectrics*, Clarendon Press, Oxford, **1958**.
30 L. Onsager, *J. Am. Chem. Soc.* **1936**, *58*, 1486.
31 C. A. Coulson, U. Danielsson, *Ark. Fys.* **1954**, *8*, 239; **1954**, *8*, 245.